a

b

Supplementary Figure 1 | Molecular formula and absorbance spectrum for paint molecules selected for their low dissociation rate with CA and the capability to remain bound to CA after denaturation, reduction and alkylation. a) sodium 4-(4-(benzyl-et-amino)-ph-azo)-2,5-di-cl-benzenesulfonate. b) 10-dioxo-4-[3-(2-sulfonatooxyethylsulfonyl) anilino] anthracene-2-sulfonate. The characteristic peak absorbance wavelengths determined above were employed for the measurement of binding kinetics shown in Figure 2.
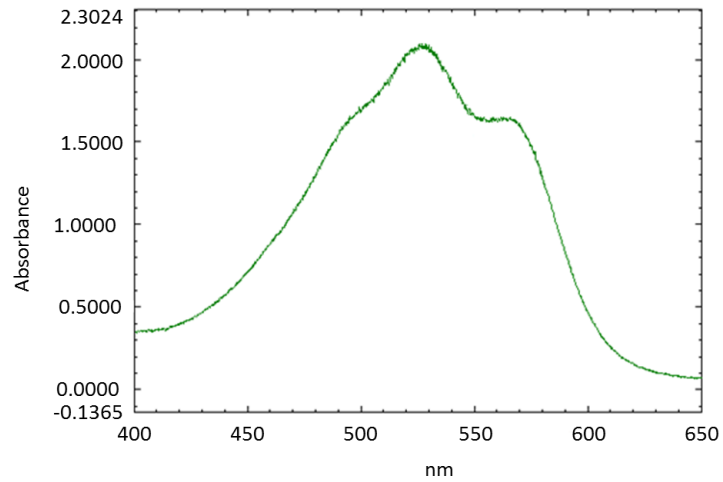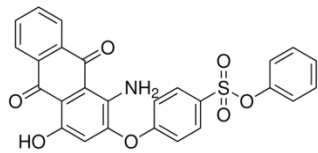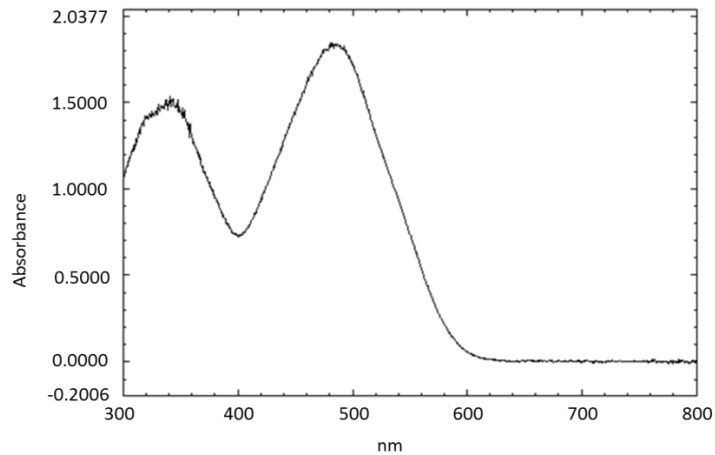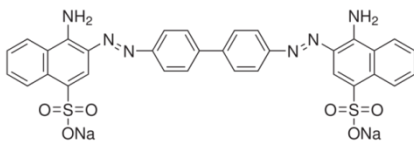
a

b

Supplementary Figure 2 | Molecular formula and absorbance spectrum for paint molecules selected for their low dissociation rate with CA and the capability to remain bound to CA after denaturation, reduction and alkylation. a) Phenyl 4-[(1-amino-4-hydroxy-9,10-dioxo-9,10-dihydro-2-anthracenyl)oxy]benzenesulfonate; and disodium; b) 4-amino-3-[[4-[4-[(1-amino-4-sulfonatonaphthalen-2-yl)diazenyl] phenyl]phenyl]diazenyl]naphthalene-1-sulfonate, respectively. The characteristic peak absorbance wavelengths determined above were employed for the measurement of binding kinetics shown in Figure 2.
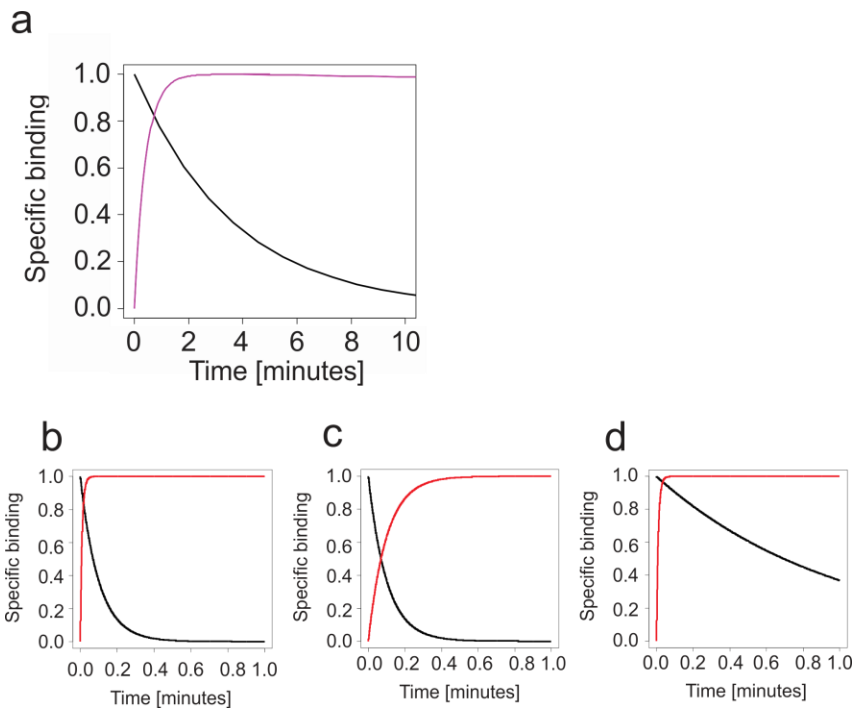
Supplementary Figure 3 | Weak transient interactions can be captured with protein painting and will not cause false positives. a) First order reaction kinetics calculations were applied in order to show that a 5 minute pulse of highly concentrated molecular paint (RBB) can cover the surface of the IL1β-IL1RI complex when most (83%) of known protein binding partners are in the complexed form. The dissociation constant for IL1 β was experimentally derived (k_{diss} = 0.252 min$^{-1;1}$) and K_d = 72*10^{-9} M. This complex is considered a strong transient complex. K_{ass}*[RBB] was experimentally derived from Figure 2 (2.4342 min^{-1}). b) Simulations show that for every protein-protein dissociation constant (k_{diss}PP), if k_{ass}MP*[MP] > k_{diss}PP of one order of magnitude, then the protein-molecular paint binding equilibrium will be reached when 83% of protein protein transient complex is still in the complexed form (P = protein, M = paint molecule, MP = protein-paint molecule complex, k_{ass}MP association constant of protein-paint molecule binding reaction). c) If k_{ass}MP*[MP] and k_{diss}PP have the same order of magnitude the protein-molecular paint binding equilibrium will be reached when 50% of protein protein transient complex is still in the complexed form. d) If k_{ass}MP*[MP] > k_{diss}PP of two orders of magnitude, then the protein-molecular paint binding equilibrium will be reached when 97% of protein protein transient complex is still in the complexed form.
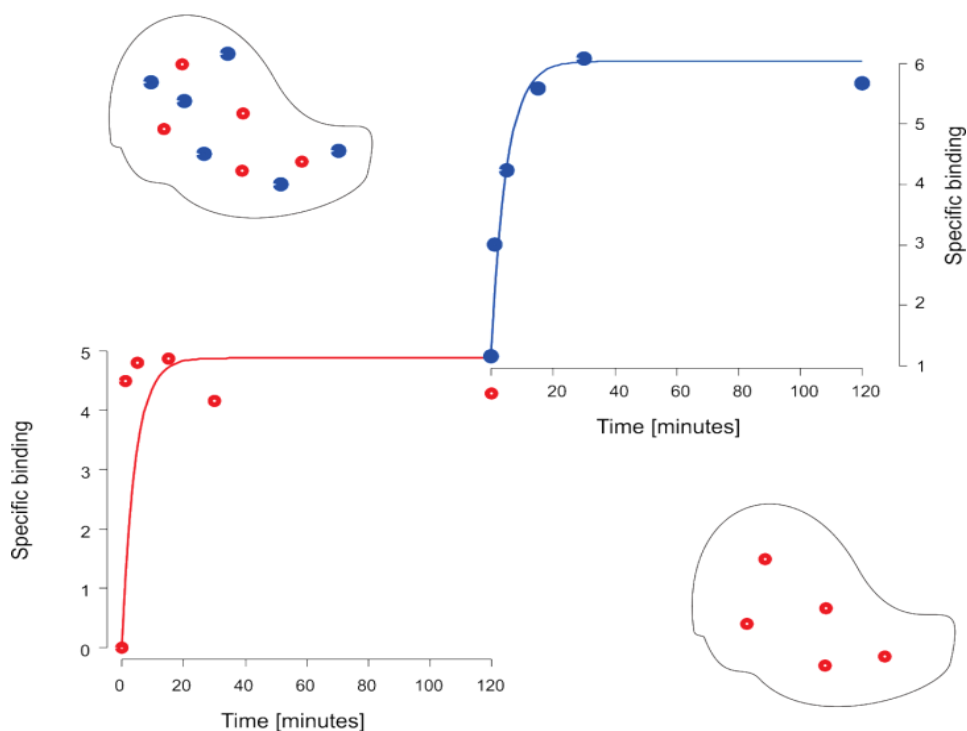
Supplementary Figure 4 | Sequential binding of two different dyes documents complementarity and rapid saturation kinetics of the dyes to achieve broad coverage of trypsin cleavage sites exposed on the surface. CA (1 nmole) and AO50 (10 nmoles) in 50 μL PBS were allowed to reach equilibrium (1 hour incubation time) and then unbound dye was separated via mini Quick Spin Oligo columns as described in the Methods. RBB (10 nmoles) was allowed to interact with AO50-painted CA for different time periods (0, 1, 5, 15, 40, and 120 minutes). Specific binding ([AO50]/[CA] and [RBB]/[CA]) was plotted against incubation times. Binding kinetics revealed that 6 moles of RBB bound to every mole of CA thus suggesting that RBB and AO50, examples of two different separate paint molecules, could bind at different regions on the protein surface.
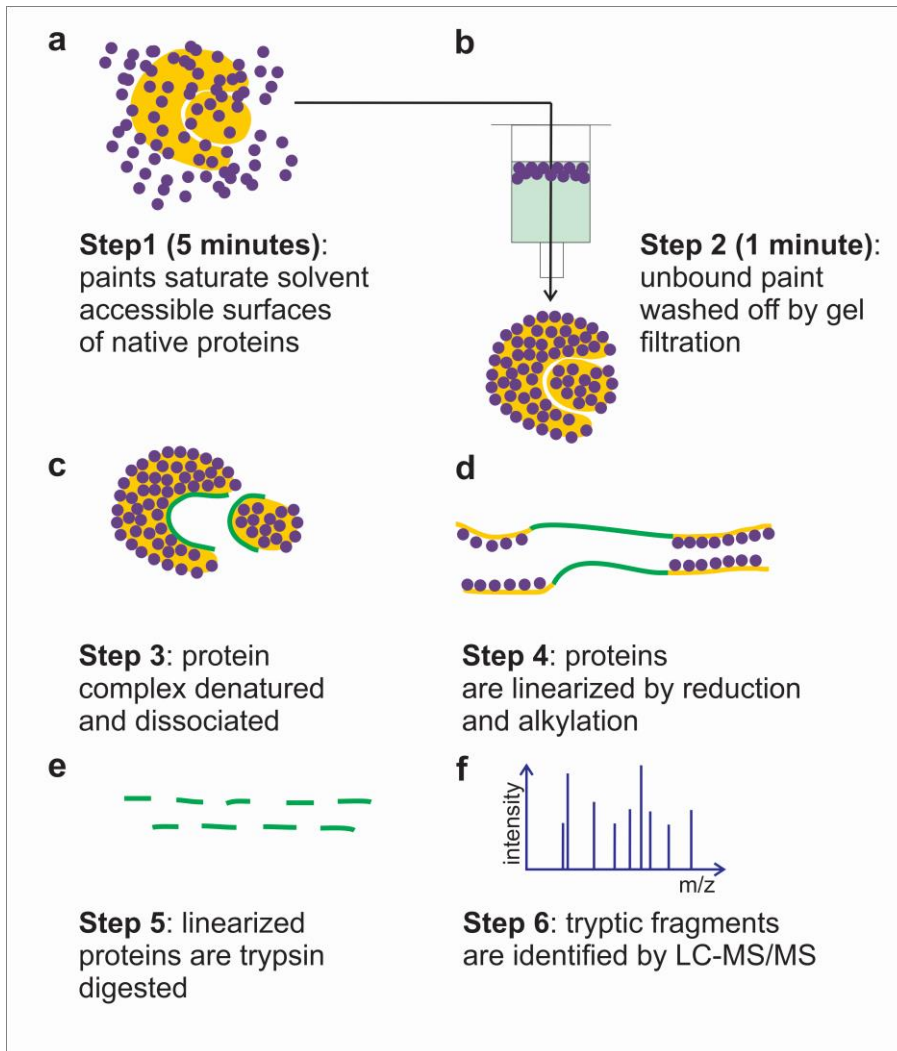
Supplementary Figure 5 | Protein painting workflow. (a) Proteins are pulsed with 10 molar excess small molecule molecular paints for 5 minutes. (b) Unbound paint molecules are washed away with gel filtration chromatography (mini Quick Spin Oligo Column, Roche). (c) The protein complex is dissociated and denatured with 2 M urea. (d) Proteins are linearized by dithiothreitol (DTT) reduction and iodoacetamide alkylation. (e) Linearized proteins are subjected to trypsin digestion. (f) Tryptic fragments are analyzed by reversed-phase liquid chromatography nanospray tandem mass spectrometry (LC-MS/MS). The bound molecular paints block trypsin cleavage sites. Therefore tryptic fragments are generated only from unpainted contact interface regions of the protein complex. After verifying that the dyes (paints) will block the trypsin cleavage sites on the protein(s) of interest, the user can then interrogate pre-formed protein complexes. As shown in Figure 4, a subset of four dyes can cover all the known trypsin consensus cleavage sites. Nevertheless, since we have not tested the dyes shown in Supplementary Table 2 against all known proteins, we are recommending that the user first confirms that the dyes will bind to their protein of interest and block the trypsin cleavage sites (Fig. 1). This step is also necessary to generate the data for differential comparison of the protein before and after complex formation.
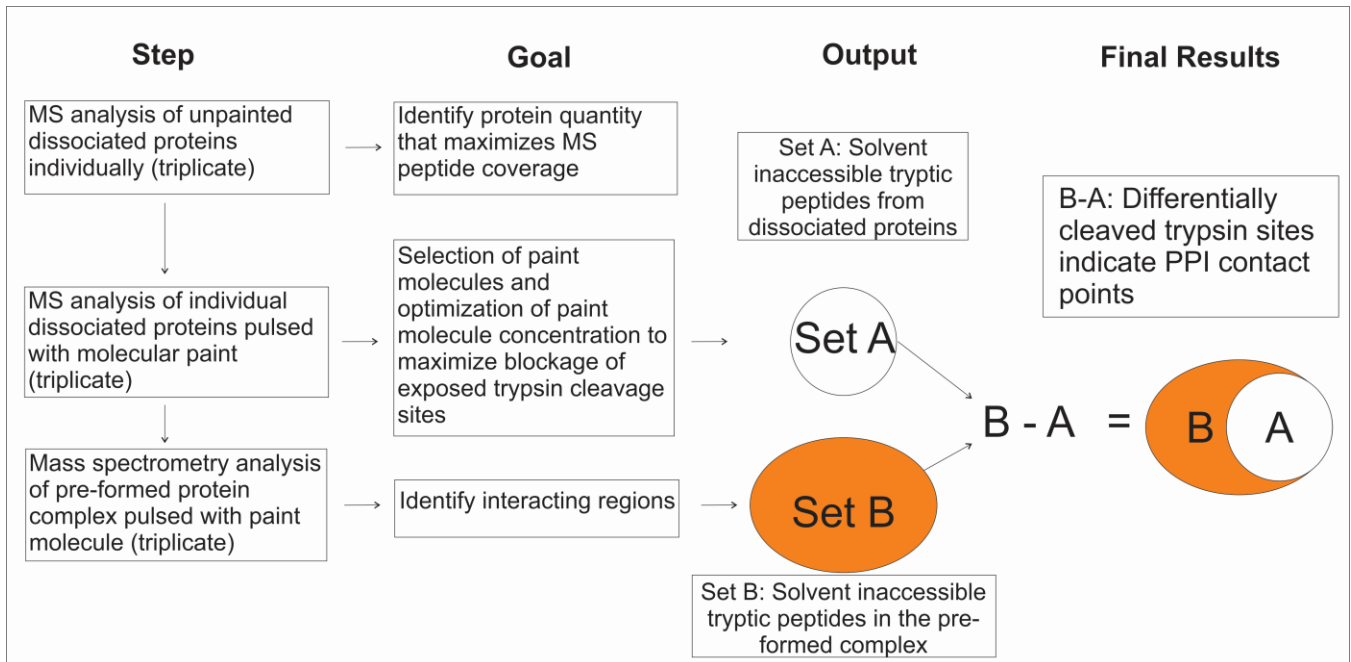
Supplementary Figure 6 | Mass spectrometry workflow. Mass spectrometry workflow steps for protein painting differentiates internal interface regions within an individual folded protein from the surface contact regions between protein partners: Step 1) Analyses of unpainted individual proteins are carried on in order to maximize the trypic peptide coverage. Step 2) Analyses of painted dissociated proteins yields a set of peptide fragments (set A) relative to solvent inaccessible trypsin cleavage sites for each individual protein 3) Analyses of the pre-formed protein-protein complex pulsed with paint molecules yields a set of peptide fragments (set B) derived from solvent inaccessible trypsin cleavage sites belonging to protein-protein interface regions. The difference between set B – set A is the output of the method. MS = mass spectrometry; PPI = protein-protein interaction.
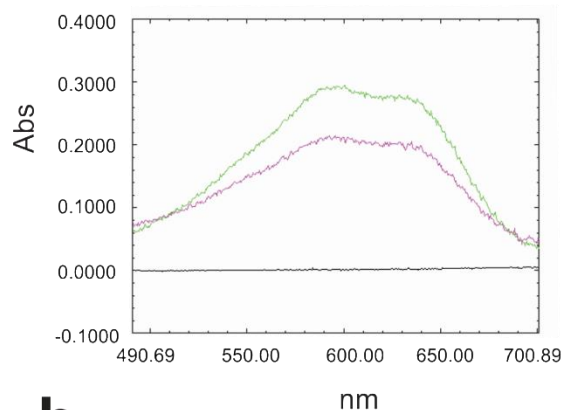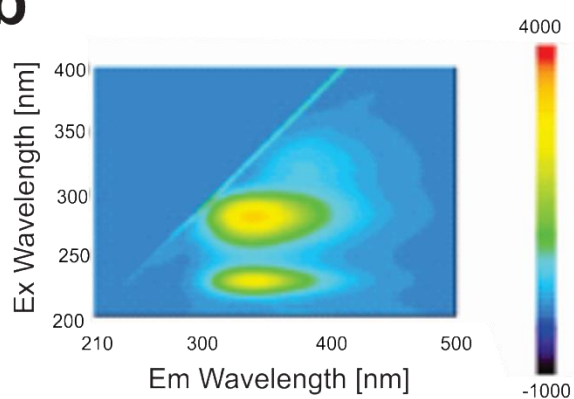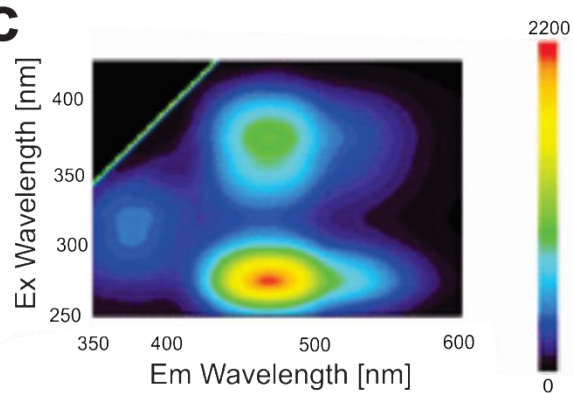
Supplementary Figure 7 | UV-VIS and fluorescence spectra of protein and paint molecules. a) Absorbance spectra are presented for CA (20 μM in PBS, black trace), RBB (40 μM in PBS, green trace) and the complex CA/RBB (20 and 40 μM respectively, magenta trace). b) 3D fluorescence spectrum of CA (10 μM in PBS). c) 3D fluorescence spectrum of ANSA (30 mM in 100% ethanol).

MSHHWGYGKHNGPEHWHKDFPIANGERQSPVDIDTKAVVQDPALKPLALVYGEAT

SRRMVNNGHSFNVEYDDSQDKAVLKDGPLTGTYRLVQFHFHWGSSDDQGSEHTV

DRKKYAAELHLVHWNTKYGDFGTAAQQPDGLAVVGVFLKVGDANPALQKVLDALD

SIKTKGKSTDFPNFDPGSLLPNVLDYWTYPGSLTTPPLLESVTWIVLKEPISVSSQQ

MLKFRTLNFNAEGEPELLMLANWRPAQPLKNRQVRGFPK

Supplementary Figure 8 | Selected molecular paints are complementary to each other and block all trypsin cleavage sites of carbonic anhydrase II. Molecular paints (RBB: blue "X", AO50: orange "X", R49: orange "X", and CR: red "X") blocked all (100%) consensus trypsin cleavage sites and showed complementarity.

IL1β

APVRSLNCTLRDSQQKSLVMSGPYELKALHLQGQDMEQQVVFSMSFVQGE
ESNDKIPVALGLKEKNLYLSCVLKDDKPTLQLESVDPKNYPKKKMEKRFVFNKI
EINNKLEFESAQFPNWYISTSQAENMPVFLGGTKGGQDITDFTMQFVSS

IL1RI

DKCKEREEKIILVSSANEIDVRPCPLNPNEHKGTITWYKDDSKTPVSTEQASRI
HQHKEKLWFVPAKVEDSGHYYCVVRNSSYCLRIKISAKFVENEPNLCYNAQAI
FKQKLPVAGDGGLVCPYMEFFKNENNELPKLQWYKDCKPLLLDNIHFSGVKD
RLIVMNVAEKHRGNYTCHASYTYLGKQYPITRVIEFITLEENKPTRPVIVSPANE
TMEVDLGSQIQLICNVTGQLSDIAYWKWNGSVIDEDDPVLGEDYYSVENPAN
KRRSTLITVLNISEIESRFYKHPFTCFAKNTHGIDAAYIQLIYPVTNFQK

Supplementary Figure 9 | Mass spectrometry identified trypsin cleavage sites within interface domains of the painted native IL1β-IL1RI complex. Interfacing residues predicted by crystal structure (PDBePISA software[2] on PDB entry 1ITB) in the IL1β-IL1RI complex are highlighted in yellow. Resolution of our protein painting method is determined by the nearest trypsin cleavage site at or near the contact point/close interface, where there is solvent exclusion, hydrogen bonds and salt bridges. Trypsin cleavage sites (R or K) revealed by protein painting followed by mass spectrometry are labeled and compared to the crystal structure predicted interfaces. All the consensus trypsin cleavage sites that were within 9 amino acids of a contact point predicted by crystal structure were correctly identified by protein painting and mass spectrometry analysis (Fisher exact test p-value = 0.0003, odds ratio = 13.49206). It's important to note that an MS peptide revealed by protein painting constitutes a true positive independent of the MS protein coverage.

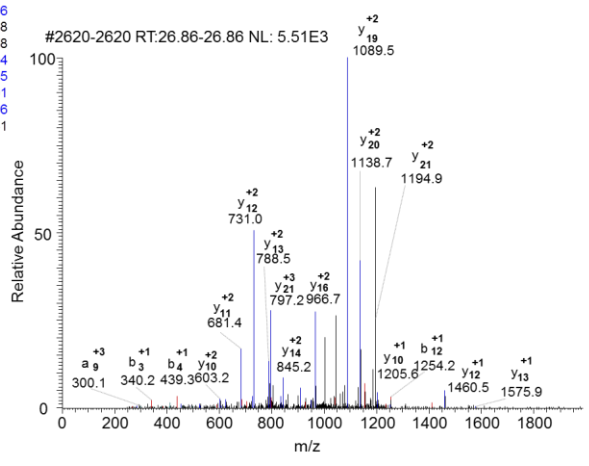| AA	A	B	Y
F	120.0807757	148.0756904	-
Y	283.1441043	311.1390189	1298.635071
K	411.2390673	439.2339819	1135.571743
H	548.2979791	576.2928937	1007.47678
P	645.350743	673.3456576	870.417868
F	792.4191569	820.4140715	773.3651042
T	893.4668353	921.4617499	626.2966903
C	1053.497515	1081.49243	525.2490118
F	1200.565929	1228.560844	365.2183318
A	1271.603043	1299.597958	218.1499179
K	-		147.1128041

Interface residue: IL1RI Lys298
Peptide: FYKHPFTCFAK
Precursor ion: 723.35068
Charge 2
Scan 1984
P(pep) 9.0E-7
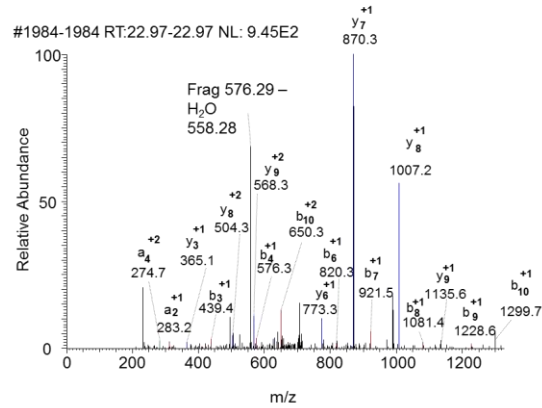
Supplementary Figure 10 | Peptide FYKHPFTCFAK identified with mass spectrometry relative to the interface regions of IL1β-IL1RI complex.

AA	A	B	Y
I	86.09642579	114.0913404	-
I	199.1804898	227.1754044	2502.276964
L	312.2645537	340.2594683	2389.1929
V	411.3329676	439.3278822	2276.108836
S	498.364996	526.3599106	2177.040422
S	585.3970244	613.391939	2090.008394
A	656.4341382	684.4290528	2002.976366
N	770.4770656	798.4719803	1931.939252
E	899.5196587	927.5145733	1817.896324
I	1012.603723	1040.598637	1688.853731
D	1127.630666	1155.62558	1575.769667
V	1226.69908	1254.693994	1460.742724
R	1382.800191	1410.795105	1361.67431
P	1479.852954	1507.847869	1205.573199
C	1639.883634	1667.878549	1108.520436
P	1736.936398	1764.931313	948.4897556
L	1850.020462	1878.015377	851.4369918
N	1964.06339	1992.058304	738.3529278
P	2061.116154	2089.111068	624.3100004
N	2175.159081	2203.153996	527.2572365
E	2304.201674	2332.196589	413.2143091
H	2441.260586	2469.255501	284.171716
K	-		147.1128041

Interface residue: IL1RI Lys12
Peptide: IILVSSANEIDVRPCPLNPNEHK
P (pep) 5.8E-11
Precursor ion 872.46216
Charge 3
Scan 2620

Supplementary Figure 11 | Peptide IILVSSANEIDVRPCPLNPNEHK identified with mass spectrometry relative to the interface regions of IL1β-IL1RI complex.

AA	A	B	Y
L	86.09642579	114.0913404	-
I	199.1804898	227.1754044	1196.6568
V	298.2489037	326.2438183	1083.5728
M	429.2893883	457.2843029	984.50436
N	543.3323157	571.3272303	853.46388
V	642.4007296	670.3956442	739.42095
A	713.4378434	741.432758	640.35253
E	842.4804365	870.4753511	569.31542
K	970.5753995	998.5703141	440.27283
H	1107.634311	1135.629226	312.17786
R	-		175.11895

Interface residue: IL1RI Arg163
Peptide: LIVMNVAEKHR
precursor ion: 655.37561
Charge 2
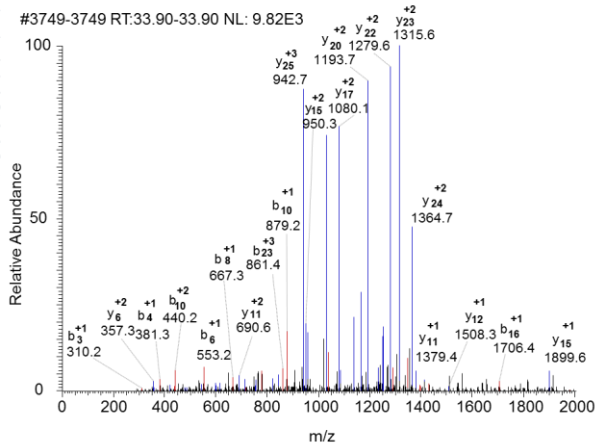P(pep) 2.2E-9
Scan 1542

#1542-1542 RT:20.28-20.28 NL: 2.16E3
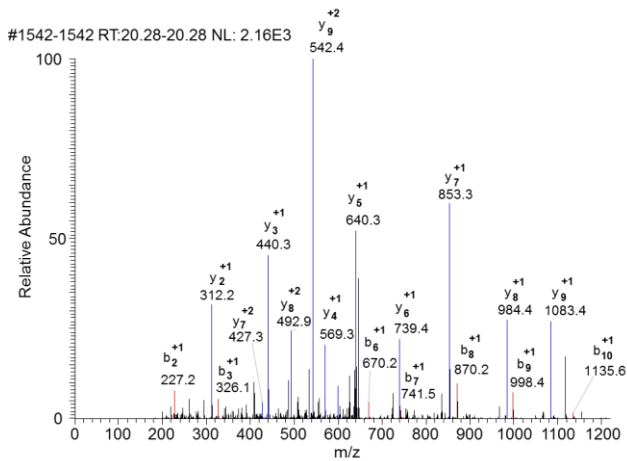
Supplementary Figure 12 | Peptide LIVMNVAEKHR identified with mass spectrometry relative to the interface regions of IL1β-IL1RI complex.

AA	A	B	Y
L	86.09642579	114.0913404	-
P	183.1491896	211.1441043	2825.327345
V	282.2176035	310.2125182	2728.274581
A	353.2547173	381.2496319	2629.206167
G	410.276181	438.2710957	2558.169053
D	525.3031241	553.2980387	2501.14759
G	582.3245878	610.3195024	2386.120647
G	639.3460515	667.3409661	2329.099183
L	752.4301155	780.4250301	2272.077719
V	851.4985294	879.493444	2158.993655
C	1011.529209	1039.524124	2059.925241
P	1108.581973	1136.576888	1899.894561
Y	1271.645302	1299.640216	1802.841797
M	1402.685786	1430.680701	1639.778469
E	1531.728379	1559.723294	1508.737984
F	1678.796793	1706.791708	1379.695391
F	1825.865207	1853.860122	1232.626977
K	1953.96017	1981.955085	1085.558563
N	2068.003098	2095.998012	957.4636004
E	2197.045691	2225.040605	843.420673
N	2311.088618	2339.083533	714.3780799
N	2425.131546	2453.12646	600.3351525
E	2554.174139	2582.169053	486.292225
L	2667.258203	2695.253117	357.2496319
P	2764.310967	2792.305881	244.165568
K	-	-	147.1128041

Interface residues: IL1RI Lys114, Lys132
Peptide: LPVAGDGGLVCPYMEFFKNENNELPK
Precursor ion 980.14722
Charge 3
Scan 3749
P(pep) 6.7E-16

Supplementary Figure 13 | Peptide LPVAGDGGLVCPYMEFFKNENNELPK identified with mass spectrometry relative to the interface regions of IL1β-IL1RI complex.

AA	A	B	Y
I	86.09642579	114.0913404	-
P	183.1491896	211.1441043	954.5982434
V	282.2176035	310.2125182	857.5454795
A	353.2547173	381.2496319	758.4770656
L	466.3387813	494.3336959	687.4399519
G	523.360245	551.3551596	574.3558879
L	636.444309	664.4392236	517.3344242
K	764.539272	792.5341866	404.2503602
E	893.581865	921.5767797	276.1553972
K	-	-	147.1128041

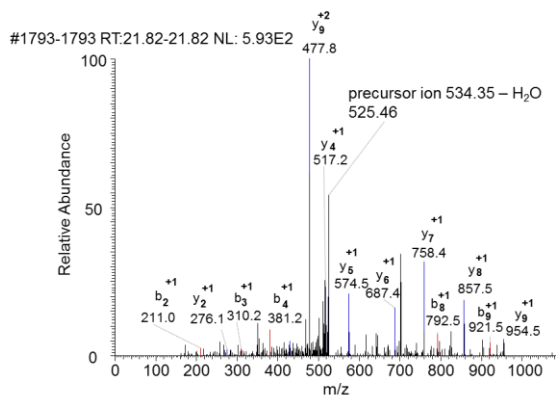Interface residue: IL1β Lys55
Peptide: IPVALGLKEK
Precursor ion 534.34576
Charge 2
Scan 1739
P(pep) 2.3E-5

Supplementary Figure 14 | Peptide IPVALGLKEK identified with mass spectrometry relative to the interface regions of IL1β-IL1RI complex.

AA	A	B	Y
S	60.04439023	88.03930485	-
L	173.1284542	201.1233688	1362.679455
N	287.1713816	315.1662963	1249.595391
C	447.2020616	475.1969763	1135.552464
T	548.2497401	576.2446547	975.521784
L	661.3338041	689.3287187	874.4741055
R	817.4349151	845.4298297	761.3900416
D	932.4618581	960.4567727	605.2889306
S	1019.493886	1047.488801	490.2619875
Q	1147.552464	1175.547379	403.2299591
Q	1275.611041	1303.605956	275.1713816
K	-		147.1128041

Interface residues: IL1β Arg4-Lys16
Peptide: SLNCTLRDSQQK
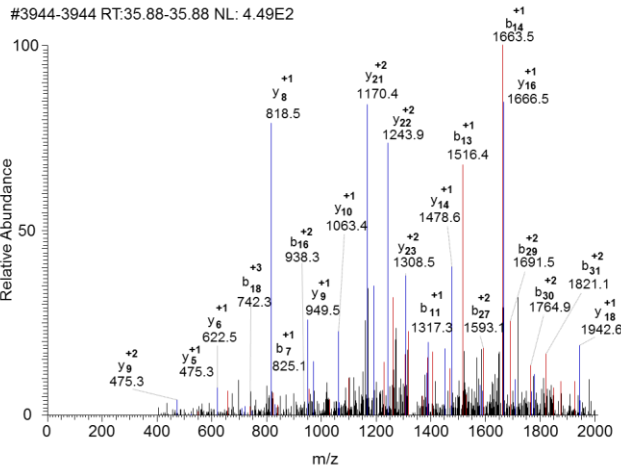Precursor ion 725.37238
Charge 2
Scan 946
P(pep) 9.1E-8
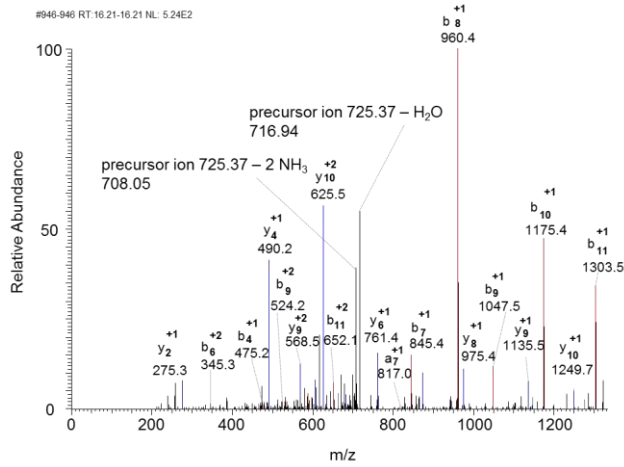
Supplementary Figure 15 | Peptide SLNCTLRDSQQK identified with mass spectrometry relative to the interface regions of IL1β-IL1RI complex.

AA	A	B	Y
I	86.09642579	114.0913404	-
E	215.1390189	243.1339335	3889.874167
I	328.2230828	356.2179975	3760.831573
N	442.2660103	470.2609249	3647.74751
N	556.3089377	584.3038523	3533.704582
K	684.4039007	712.3988153	3419.661655
L	797.4879647	825.4828793	3291.566692
E	926.5305578	954.5254724	3178.482628
F	1073.598972	1101.593886	3049.440035
E	1202.641565	1230.636479	2902.371621
S	1289.673593	1317.668508	2773.329028
A	1360.710707	1388.705622	2686.296999
Q	1488.769284	1516.764199	2615.259885
F	1635.837698	1663.832613	2487.201308
P	1732.890462	1760.885377	2340.132894
N	1846.93339	1874.928304	2243.08013
W	2033.012703	2061.007617	2129.037203
Y	2196.076031	2224.070946	1942.95789
I	2309.160095	2337.15501	1779.894561
S	2396.192123	2424.187038	1666.810497
T	2497.239802	2525.234716	1579.778469
S	2584.27183	2612.266745	1478.73079
Q	2712.330408	2740.325322	1391.698762
A	2783.367522	2811.362436	1263.640185
E	2912.410115	2940.405029	1192.603071
N	3026.453042	3054.447957	1063.560478
M	3157.493527	3185.488441	949.5175503
P	3254.546291	3282.541205	818.4770656
V	3353.614704	3381.609619	721.4243018
F	3500.683118	3528.678033	622.3558879
L	3613.767182	3641.762097	475.287474
G	3670.788646	3698.783561	362.20341
G	3727.81011	3755.805024	305.1819463
T	3828.857788	3856.852703	248.1604826
K	-		147.1128041

Interface residue: IL1β Lys103

Peptide:
IEINNKLEFESAQFPNWYISTSQAENMPVFLGGTK

Precursor ion 1334.99622

Charge 3

Scan 3944

P(pep) 1.5E-12

#3944-3944 RT:35.88-35.88 NL: 4.49E2

Supplementary Figure 16 | Peptide IEINNKLEFESAQFPNWYISTSQAENMPVFLGGTK identified with mass spectrometry relative to the interface regions of IL1β-IL1RI complex.

Interface residue: IL1β Lys109
Peptide LEFESAQFPNWYISTSQAENMPVFLGGTK
Precursor ion 1097.86499
Charge 3
Scan 4037
P(pep) 4.1E-13

AA	A	B	Y
L	86.09642579	114.0913404	-
E	215.1390189	243.1339335	3178.482628
F	362.2074328	390.2023474	3049.440035
E	491.2500259	519.2449405	2902.371621
S	578.2820543	606.2769689	2773.329028
A	649.319168	677.3140827	2686.296999
Q	777.3777455	805.3726602	2615.259885
F	924.4461594	952.4410741	2487.201308
P	1021.498923	1049.493838	2340.132894
N	1135.541851	1163.536765	2243.08013
W	1321.621164	1349.616078	2129.037203
Y	1484.684492	1512.679407	1942.95789
I	1597.768556	1625.763471	1779.894561
S	1684.800585	1712.795499	1666.810497
T	1785.848263	1813.843178	1579.778469
S	1872.880291	1900.875206	1478.73079
Q	2000.938869	2028.933784	1391.698762
A	2071.975983	2099.970897	1263.640185
E	2201.018576	2229.01349	1192.603071
N	2315.061503	2343.056418	1063.560478
M	2446.101988	2474.096902	949.5175503
P	2543.154752	2571.149666	818.4770656
V	2642.223166	2670.21808	721.4243018
F	2789.291579	2817.286494	622.3558879
L	2902.375643	2930.370558	475.287474
G	2959.397107	2987.392022	362.20341
G	3016.418571	3044.413485	305.1819463
T	3117.466249	3145.461164	248.1604826
K	-		147.1128041

#4037-4037 RT:36.72-36.72 NL: 6.94E2
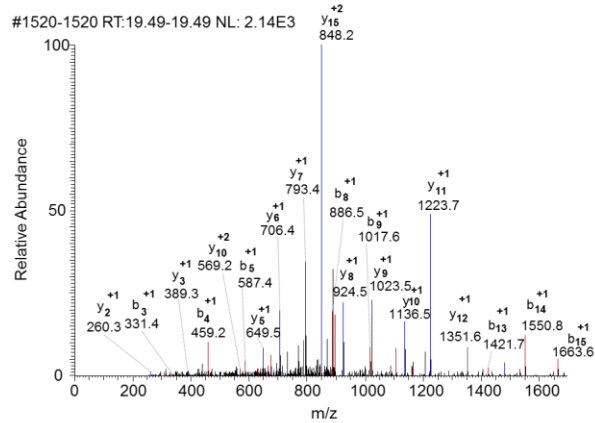
Supplementary Figure 17 | Peptide LEFESAQFPNWYISTSQAENMPVFLGGTK identified with mass spectrometry relative to the interface regions of IL1β-IL1RI complex.

AA	A	B	Y
D	88.03930485	116.0342195	-
S	175.0713333	203.0662479	1694.878183
Q	303.1299108	331.1248254	1607.846155
Q	431.1884883	459.1834029	1479.787577
K	559.2834513	587.2783659	1351.729
S	646.3154797	674.3103943	1223.634037
L	759.3995436	787.3944582	1136.602008
V	858.4679575	886.4628721	1023.517944
M	989.5084421	1017.503357	924.4495303
S	1076.540471	1104.535385	793.4090457
G	1133.561934	1161.556849	706.3770173
P	1230.614698	1258.609613	649.3555535
Y	1393.678027	1421.672941	552.3027897
E	1522.72062	1550.715534	389.2394612
L	1635.804684	1663.799598	260.1968681
K	-		147.1128041

Interface residues: IL1β Arg11-Lys27
Peptide DSQQKSLVMSGPYELK
Precursor ion 905.46307
Charge 2
Scan 1520
P(pep) 1.2E-11

Supplementary Figure 18 | Peptide DSQQKSLVMSGPYELK identified with mass spectrometry relative to the interface regions of IL1β-IL1RI complex.

Hotspot residue: IL1RAcP Arg286

Peptide: TEDETRTQILSIK

Precursor ion 767.40955

Charge 2

P(pep) 7.2E-5

scan 1492

#1492-1492 RT:19.87-19.87 NL: 3.50E1

prec 767.40 – 2 NH$_3$
750.12

y_{11}^{+2} 652.7

b_{10}^{+1} 1187.5

y_{10}^{+1} 1188.6

b_{11}^{+1} 1274.8

b_{12}^{+1} 1387.9

b_{6}^{+1} 732.3

b_{9}^{+1} 1074.6

b_{8}^{+1} 961.5

y_{10}^{+2} 595.0

y_{9}^{+2} 530.6

y_{8}^{+1} 958.6

b_{3}^{+1} 346.2

y_{3}^{+1} 347.4

y_{4}^{+1} 460.0

Relative Abundance

m/z
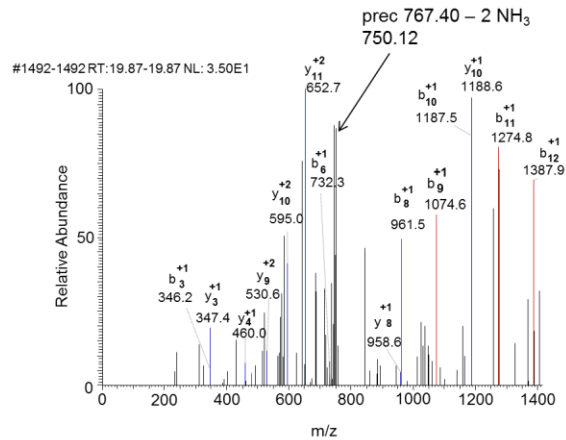
Supplementary Figure 19 | Arg286 peptide mass spectrometry sequence. IL1RAcP peptide identified by protein painting followed by mass spectrometry relative to the closest proximity hot spot in the IL1β-IL1RI-IL1RAcP complex. Protein painting revealed this single region as an interaction point incorporating an arginine at the outermost bend of the beta loop and was predicted to participate both in hydrogen bonding and salt bridge formation between the accessory protein and the receptor-ligand complex. This peptide was used to generate Arg 286 peptide inhibitor and was also used as the antigen for Arg286 pep monoclonal antibody production (Fig. 6).
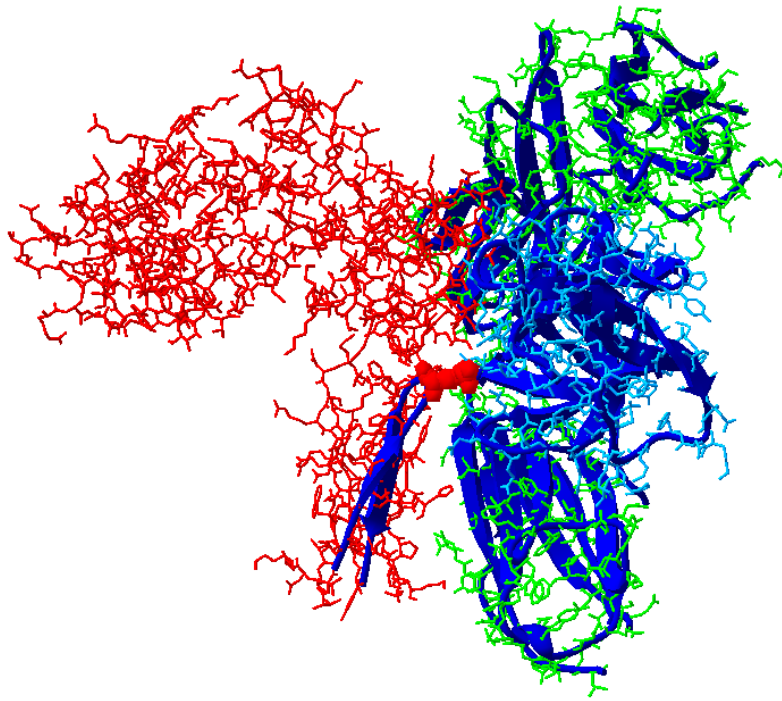
Supplementary Figure 20 | Arg286 peptide 3D model. Arg 286 peptide is represented as a ribbon structure in the context of the ternary complex. Arg286 amino acid is represented by solid spheres. IL1RAcP is depicted in the red backbone.

Species	Start	Sequence	End
Arg286 pep	1	T I N E S I S H S R T E D E T R T Q I L S	21
Homo sapiens	156	T I N E S I S H S R T E D E T R T Q I L S	176
Macaca mulatta	297	T I N E S I S H S R T E D E T R T Q I L S	317
Pongo abelii	297	T I N E S I S H S R T E D E T R T Q I L S	317
Callithrix jacchus	297	T I N E S I S H S R T E D E T R T Q I L S	317
Pan troglodytes	297	T I N E S I S H S R T E D E T R T Q I L S	317
Gorilla gorilla	294	T I N E S I S H S R T E D E T R T Q I L S	314
Nomascus leucogenys	297	T I N E S I S H S R T E D E T R T Q I L S	317
Spermophilus tridecemlineatus	298	T I N E S I S Y T K T E D E T R T Q I L S	318
Rattus norvegicus	156	T I N E S V S Y S S T E D E T R T Q I L S	176
Mus musculus	297	T I N E S V S Y S S T E D E T R T Q I L S	317
Otolemur garnettii	290	T I N E S I S L T R T E D E M R T Q I L S	309
Mustela putorius	62	T V N E S I S L T Q T E D E T R T Q I L N	82
Oryctolagus cuniculus	296	T I N E S L S Y S K T E D E T R T H V L S	316
Felis catus	299	T V N E S I S L T T T E D E T R T Q V L S	319
Sus scrofa	295	S I N E S V S L S K I E D E T R T Q L L S	315
Cricetulus griseus	298	T T N E S V S Y S T T E D E T R T Q I L S	317
Heterocephalus glaber	297	T I S E S T S Y S K T E D E T R T Q V L S	317
Pteropus alecto	465	T I N E S V S Q T K T E D E K R T Q V L S	484
Canis familiaris	299	T V N E S V S L T A T E D E M R T Q I L N	319
Cavia porcellus	293	T I S E S A S Y S T M E D E T R T Q V L S	313
Bos taurus	297	S V N E S V I L K V T E D E T R T Q L L S	317

Supplementary Figure 21 | Arg286 peptide sequence conserved in evolution. Sequence of Arg286 peptide found by protein painting is compared among species. Identical residues are shown in dark green. This peptide sequence is conserved in evolution reflecting its important functional role[3]. The numbers flanking the sequences are those provided by BLASTp software.
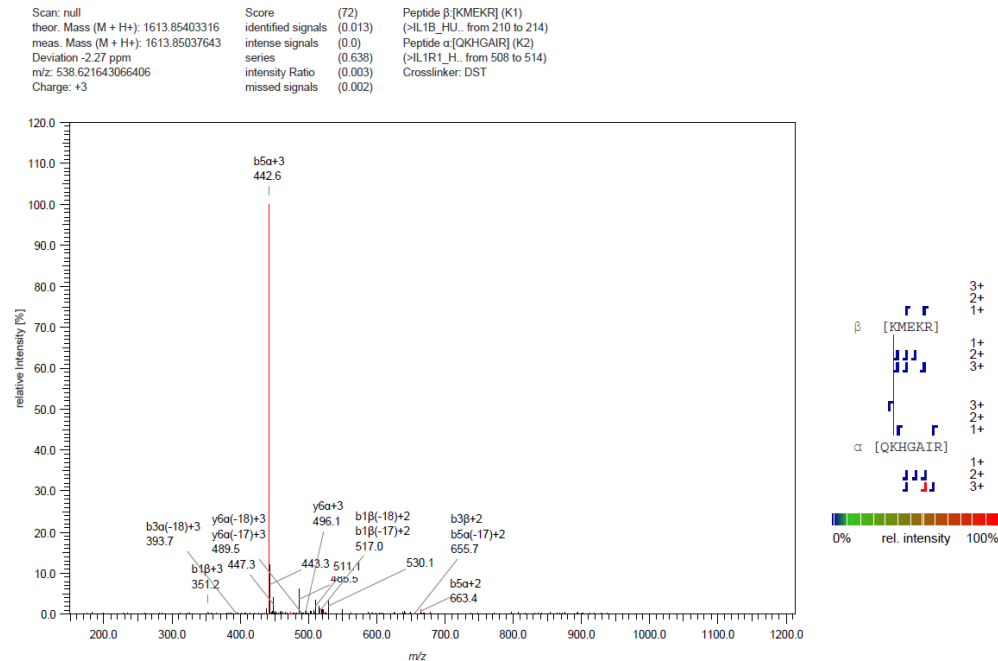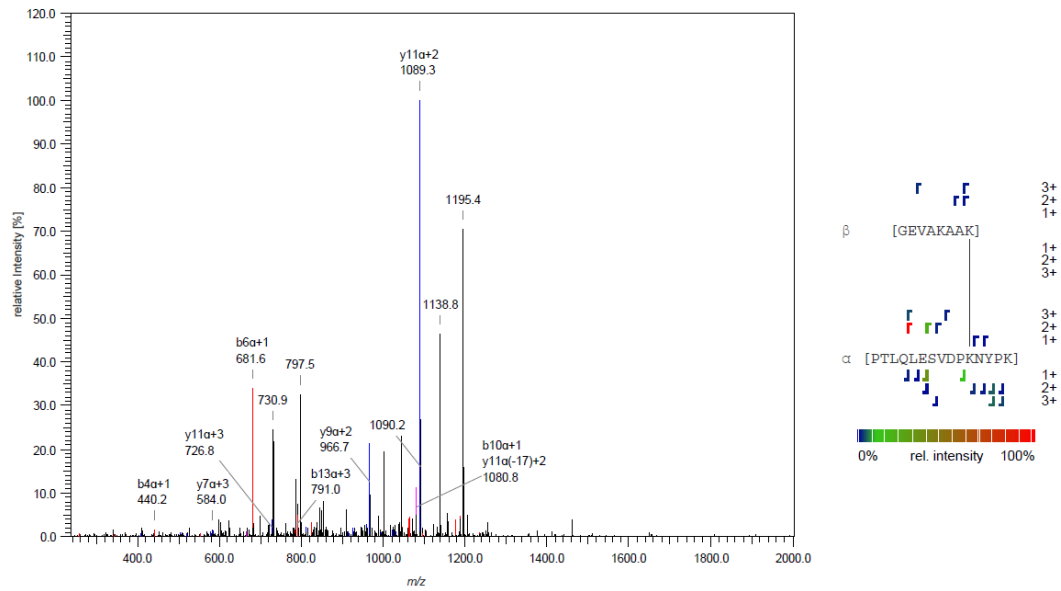
Supplementary Figure 22 | Experimental spectrum obtained with the crosslinking method applied to the 3-way IL1β complex. DST and sulfo-EGS were used to form covalent crosslinks in the pre-formed IL1β-IL1RI-IL1RAcP complex. The cross linking reactions was allowed to proceed for 30 and 120 minutes (2 crosslinkers × 2 time periods = 4 conditions). Proteins were denatured, trypsin digested, desalted and analyzed with mass spectrometry (See Methods section). Data analysis was performed with StavroX[4]. Cross-link identifications were filtered by requiring a score > 20. Experimental spectrum obtained for cross-linked peptide 1 listed in Supplementary Table 8.

Supplementary Figure 23 | Experimental spectrum obtained with the crosslinking method applied to the 3-way IL1β complex. Experimental spectrum obtained for cross-linked peptide 2 listed in Supplementary Table 8.

Scan: null
theor. Mass (M + H+): 2631.35120159
meas. Mass (M + H+): 2631.34622604
Deviation -1.89 ppm
m/z: 877.786926269531
Charge: +3

Score   (20)
identified signals   (0.491)
intense signals   (0.734)
series   (0.031)
intensity Ratio   (0.691)
missed signals   (0.827)

Peptide β:[SAKGEVAK] (K3)
(>IL1AP_H.. from 335 to 342)
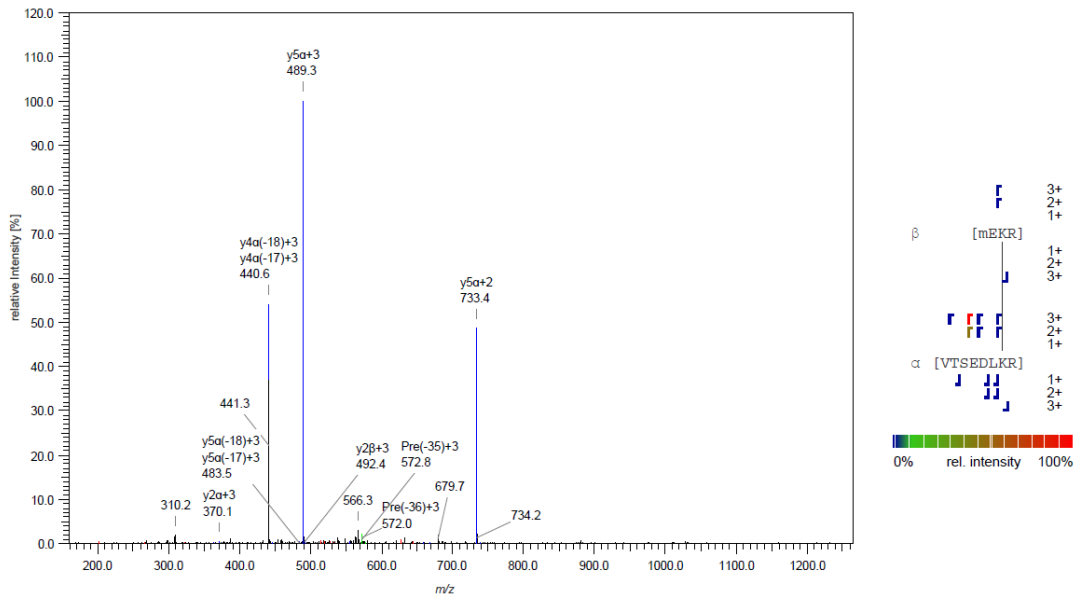Peptide α:[PTLQLESVDPKNYPK] (K11)
(>IL1B_HU.. from 194 to 208)
Crosslinker: DST
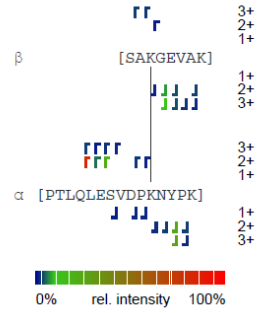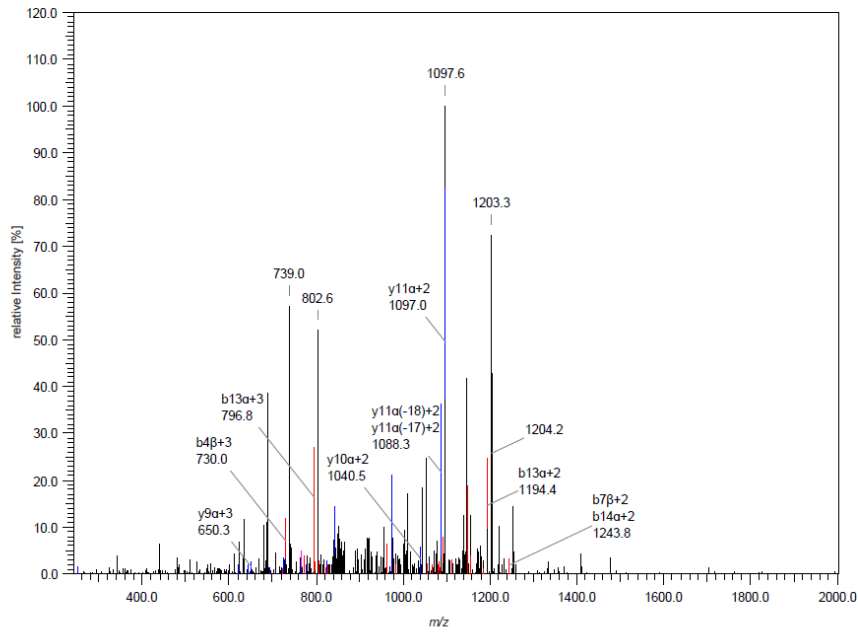
Supplementary Figure 24 | Experimental spectrum obtained with the crosslinking method applied to the 3-way IL1β complex. Experimental spectrum obtained for cross-linked peptide 3 listed in Supplementary Table 8.

Scan: null
theor. Mass (M + H+): 1751.84800414
meas. Mass (M + H+): 1751.84305222
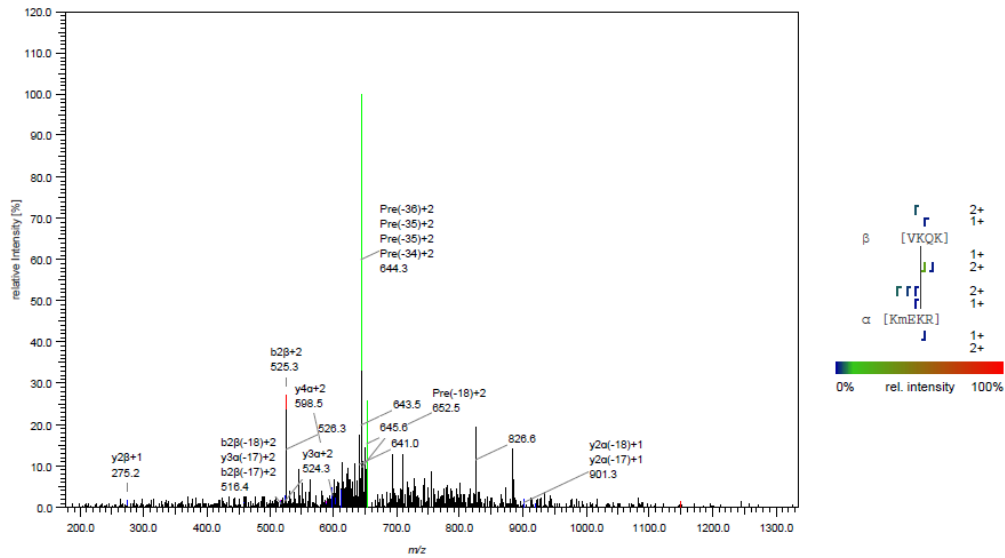Deviation -2.83 ppm
m/z: 584.619201660156
Charge: +3

Score   (58)
identified signals (0.104)
intense signals   (0.005)
series   (0.45)
intensity Ratio   (0.452)
missed signals   (0.01)

Peptide β:[mEKR] (K3)
(>IL1B_HU.. from 211 to 214)
Peptide α:[VTSEDLKR] (K7)
(>IL1AP_H.. from 320 to 327)
Crosslinker: sulfoEGS

Supplementary Figure 25 | Experimental spectrum obtained with the crosslinking method applied to the 3-way IL1β complex. Experimental spectrum obtained for cross-linked peptide 4 listed in Supplementary Table 8.
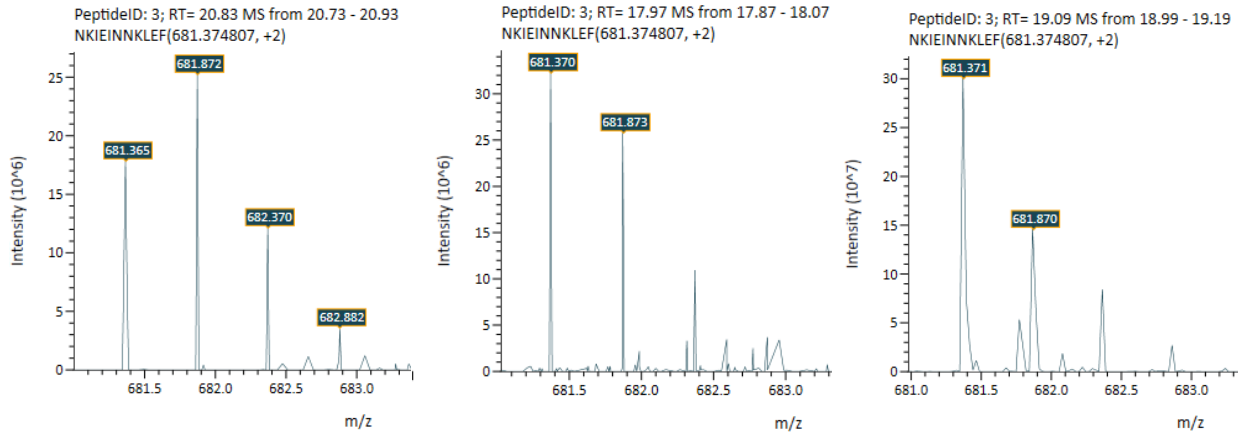
Supplementary Figure 26 | Experimental spectrum obtained with the crosslinking method applied to the 3-way IL1β complex. Experimental spectrum obtained for cross-linked peptide 5 listed in Supplementary Table 8.
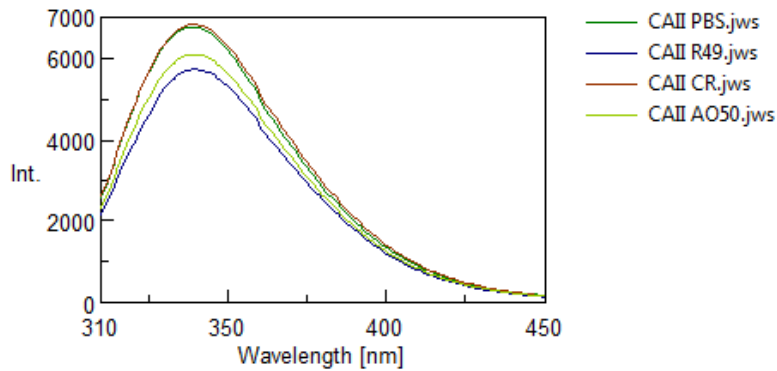
Supplementary Figure 27 | Results of the hydrogen/deuterium exchange method applied to the 3-way IL1β complex. Deuterium off-exchange experiments were performed on the 3-way IL1β complex (see Methods section). Example mass spectra of the NKIEINNKLEF peptic fragments (IL1β) in the unbound, bound and unlabeled condition from left to right.
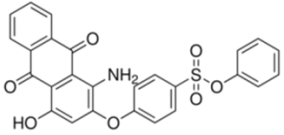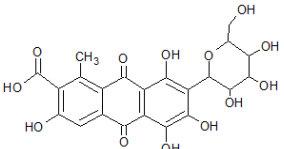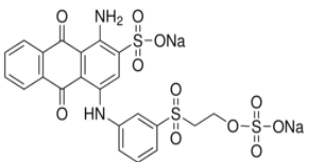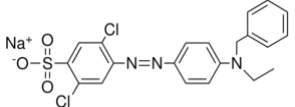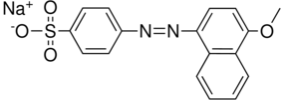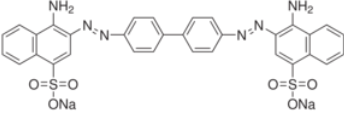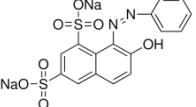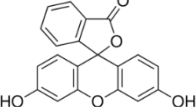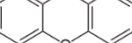
Supplementary Figure 28 | Fluorescence emission spectra of CA bound to different dyes show no shift in the maximum peak with respect to CA in PBS. A solution of 10 mM CA in PBS was subjected to fluorescence spectroscopy. Intrinsic protein fluorescence is due to aromatic amino acids, predominantly tryptophan. The excitation wavelength (λex) was set at 295 nm because at this wavelength there is no absorption by tyrosine. The emission spectrum was recorded with Jasco Spectrofluorometer FP-8300 and analyzed with Jasco Spectra Manager Version 2. The emission spectra (λex = 295nm) was recorded for CA pulsed for 5 minutes with the following example dyes: R49, CR, AO50 and immediately passed through Sephadex columns in order to eliminate unbound dye Supplementary Figure 5). No shift in the maximum emission peak (340 nm) was evident. This suggests that solvent accessibility of (7) tryptophan residues in CA is not modified. Therefore no modification in the three dimensional conformation (involving tryptophan residues) of the protein occurs after a short pulse of dyes.
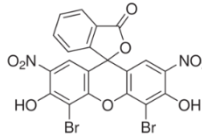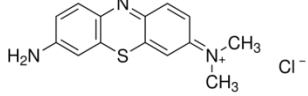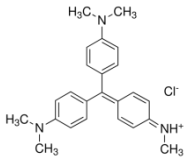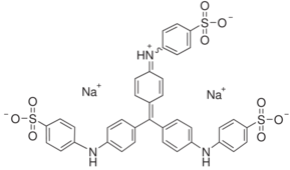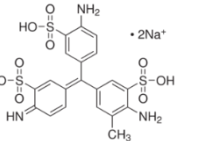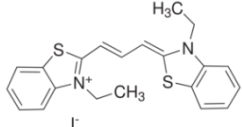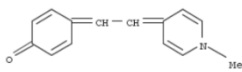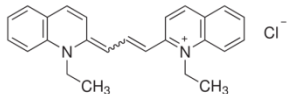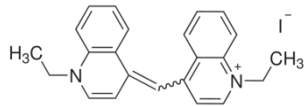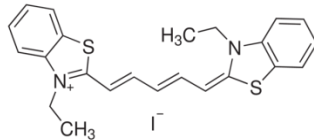
Supplementary Table 1: Paint molecules selected for their low dissociation rate with CA and the capability to remain bound to CA after denaturation, reduction and alkylation
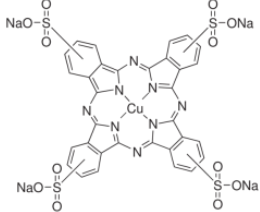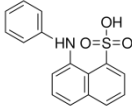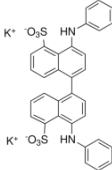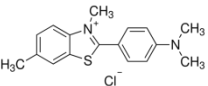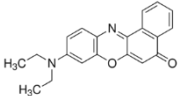
	Chemical Name (abbreviation)	MW	k_{off} [10^{-5} s^{-1}]	Bound after CA reduction and alkylation	Water soluble
1	sodium 4-(4-(benzyl-et-amino)-ph-azo)-2,5-di-cl-benzenesulfonate (AO50)	486.356	5.725	Y	Y
2	disodium;1-amino-9, 10-dioxo-4-[3-(2-sulfonatooxyethylsulfonyl)anilino]anthracene-2-sulfonate (RBB)	626.54	3.222	Y	Y
3	phenyl 4-[(1-amino-4-hydroxy-9,10-dioxo-9,10-dihydro-2-anthracenyl)oxy]benzenesulfonate (R49)	487.492	5.899	Y	Y
4	disodium;4-amino-3-[[4-[4-[(1-amino-4-sulfonatonaphthalen-2-yl)diazenyl] phenyl]phenyl]diazenyl]naphthalene-1-sulfonate (CR)	696.66	2.538	Y	Y

Chemical properties of the paint molecules, including chemical name, molecular weight, dissociation rate, capability to remain bound to CA after reduction and alkylation, solubility in water for selected paint molecules. Selection criteria for paint molecules include: $k_{off} < 6*10^{-5}$ s^{-1}, water soluble = yes, survives to reduction and alkylation = yes. These dyes have not been previously explored for protein binding kinetics and protein cleavage site blockage.

Supplementary Table 2 : Small molecule molecular "paints" screened for use in protein painting methodology.

Class	CAS number	Name	Formula
Anthraquinone	5517-38-4	phenyl 4-[(1-amino-4-hydroxy-9,10-dioxo-9,10-dihydro-2-anthracenyl)oxy]benzenesulfonate	
Anthraquinone	1390-65-4	3,5,6,8-tetrahydroxy-1-methyl-9,10-dioxo-7-[3,4,5-trihydroxy-6-(hydroxymethyl)oxan-2-yl]anthracene-2-carboxylic acid	
Anthraquinone	2580-78-1	disodium;1-amino-9, 10-dioxo-4-[3-(2-sulfonatooxyethylsulfonyl)anilino]anthracene-2-sulfonate	
Aryl azo compound	10214-07-0	Sodium 4-(4-(benzyl-et-amino)-ph-azo)-2,5-di-cl-benzenesulfonate	
Aryl azo compound	68806-22-4	Sodium 4-[(4-methoxy-1-naphthyl)diazenyl]benzenesulfonate	
Aryl azo compound	573-58-0	disodium;4-amino-3-[[4-[4-[(1-amino-4-sulfonatonaphthalen-2-yl)diazenyl] phenyl]phenyl]diazenyl]naphthalene-1-sulfonate	
Aryl azo compound	1936-15-8	7-Hydroxy-8-phenylazo-1,3-naphthalenedisulfonic acid disodium salt	
Xanthene	2321-07-5	3',6'-dihydroxy-Spiro[isobenzofuran-1(3H),9'-[9H]xanthen]-3-one	
Xanthene	92-83-1	Xanthene	

Xanthene	548-24-3	4',5'-dibromo-3',6'-dihydroxy-2',7'-dinitro- spiro[isobenzofuran-1(3H),9'-[9H]xanthen]-3-one	
Thiazine	531-53-3	3-amino-7-(dimethylamino)-Phenothiazin-5-ium, chloride	
Triarylmethane compound	8004-87-3	N-(4-{bis[4-(dimethylamino)phenyl]methylene}-2,5-cyclohexadien-1-ylidene)methanaminium chloride	
Triarylmethane compound	28983-56-4	[[4-[bis[4-[(sulfophenyl)amino]phenyl]methylene]-2,5-cyclohexadien-1-ylidene]amino]-Benzenesulfonic acid, sodium salt (1:2)	
Triarylmethane compound	3244-88-0	2-amino-5-[(4-amino-3-sulfophenyl)(4-imino-3-sulfo-2,5-cyclohexadien-1-ylidene)methyl]-3-methyl-Benzenesulfonic acid, sodium salt	
Polymethine compound	905-97-5	3,3'-Diethylthiacarbocyanine iodide	
Polymethine compound	23302-83-2	4-[2-(1-methyl-4(1H)-pyridinylidene)ethylidene]-2,5-Cyclohexadien-1-one,	
Polymethine compound	2768-90-3	(2E)-1-ethyl-2-[(E)-3-(1-ethylquinolin-1-ium-2-yl)prop-2-enylidene] quinoline; chloride	
Polymethine compound	4727-49-5	1,1'-Diethyl-4,4'-cyanine iodide	
Polymethine compound	514-73-8	3-Ethyl-2-[5-(3-ethyl-2(3H)-benzothiazolylidene)-1,3-pentadienyl]benzothiazolium iodide	

Class	CAS number	Name	Molecular formula
Polymethine compound		Copper(II) phthalocyanine-tetrasulfonic acid tetrasodium salt	
Naphthalene derivative	82-76-8	8-Anilino-1-naphthalenesulfonic acid	
Naphthalene derivative	65664-81-5	4,4'-Dianilino-1,1'-binaphthyl-5,5'-disulfonic acid dipotassium salt	
Heterocyclic compound	2390-54-7	Thioflavine T	
Heterocyclic compound	2390-54-7	2-[4-(dimethylamino)phenyl]-3,6-dimethyl-Benzothiazolium, chloride	

Class, CAS number, name and molecular formula are shown. All molecular paints were purchased from Sigma except compounds CAS 514-73-8 and 8004-87-3 which were purchased from Fisher and CAS 2580-78-1 which was purchased from Acros Organics. Binding mechanisms involve hydrophobic and electrostatic forces[5]. Small molecular paints may preferentially recognize charged amino acids[6] predominantly found on the surface of proteins and are essential to trypsin cleavage sites. Small molecular "paints" can insert aromatic rings into non-polar hydrophobic pockets of the protein surface, while the flanking portions of the dye and protein molecules can re-arrange depending on energy constraints[5]. A variety of chemical classes (first column) were ranked for utility as molecular paints based on the following criteria using the workflow described in Supplementary Table 1: a) extremely rapid on-rates (M^{-1} sec^{-1}) and very slow off-rates (sec^{-1}), b) remain bound following protein dissociation or denaturation with 2 M urea, and c) bind to multiple sites on the exposed protein surface to achieve full coverage of all the trypsin cleavage sites.

Supplementary Table 3: Contingency table comparing protein painting positives to Robetta hotspot energy prediction model.

	Robetta +	Robetta -	Total		
PP +	8	2	10	0.8	PP Precision
PP -	9	63	72	0.88	PP Negative predictive value
Total	17	65	82		
	0.47	0.97			
	PP Sensitivity	PP Specificity			

Agreement was considered in the case a positive proteolytic fragment identified with protein painting contained a hotspot residue predicted by Robetta. PP+ = protein painting positive, PP- = protein painting negative, Robetta + = interface residue with $\Delta\Delta G >= 1.0$ kcal mol^{-1} = hotspot. Robetta - = interface residue with $\Delta\Delta G < 1.0$ kcal mol^{-1} = not a hotspot. Accuracy, calculated as *TP+TN/(TP+TN+FP+FN),* is 87%.

Supplementary Table 4: Contingency table comparing protein painting positives to KFC2 hotspot energy predictions

	KFC2 +	KFC2 -	Total		
PP +	9	1	10	0.90	PP Precision
PP -	10	62	72	0.86	PP Negative predictive value
Total	19	63	82		
	0.47	0.98			
	PP Sensitivity	PP Specificity			

Agreement was considered in the case a positive proteolytic fragment identified with protein painting contained a hotspot residue predicted by KFC2. PP+ = protein painting positive, PP- = protein painting negative, KFC2 + = interface residue predicted to be hotspot by the model. KFC2 - = interface residue predicted not to be a hotspot by the model.

Supplementary Table 5: Contingency table comparing protein painting positives to Hotpoint hotspot energy prediction model.

	Hotpoint +	Hotpoint -	Total		
PP +	8	2	10	0.8	PP Precision
PP -	9	63	72	0.88	PP Negative predictive value
Total	17	65	82		
	0.47	0.97			
	PP Sensitivity	PP Specificity			

Agreement was considered in the case a positive proteolytic fragment identified with protein painting contained a hotspot residue predicted by Hotpoint. PP+ = protein painting positive, PP- = protein painting negative, Hotpoint + = interface residue predicted to be hotspot by the model. Hotpoint - = interface residue predicted not to be a hotspot by the model.

Supplementary Table 6: Output of Robetta, KFC2 and Hotpoint prediction methods. Interface residue count is reported for Hotspot and non hotspots.

	Robetta	KFC2	Hotpoint
Hotspot	32	49	40
Non Hotspot	95	125	63
Total	127	250	103

Total residues belonging to the interface according to PDBePISA (PDB# 4DEP) = 202

Supplementary Table 7: Contingency table comparing protein painting positives to hotspots common to Robetta, Hotspot and KFC2.

	Software +	Software -	Total		
PP +	5	5	10	0.50	PP Precision
PP -	4	68	72	0.94	PP Negative predictive value
Total	9	73	82		
	0.56	0.93			
	PP Sensitivity	PP Specificity			

Agreement was considered in the case a positive proteolytic fragment identified with protein painting contained a hotspot residue predicted by Robetta, Hotspot and KFC2. PP+ = protein painting positive, PP- = protein painting negative, Software + = hotspot predicted by all three software. Software - = not a hotspot in at least one of the three prediction computational methods.

Supplementary Table 8: Results of the crosslinking method applied to the 3-way IL1β complex.

Score	Hotspot	Peptides	Crosslinked amino acid (I)	Crosslinked amino acid (A)	m/z	z	Mass calc.	Dev(ppm)
72	n	mEKR(M95_R98) / ISKEK(I72_K76)	K97	K74	538.622	3	1613.854	-2.27
38	n	PTLQLESVDPKNYPK (P78-K92) / GEVAKAAK (G319-K326)	K88	K323	872.457	3	2615.356	0.59
20	n	PTLQLESVDPKNYPK (P78-K92) / SAKGEVAK (S316-K323)	K88	K318	877.787	3	2631.351	-1.89
58	n	mEKR (M95-R98) / VTSEDLKR (V301-R308)	K97	K307	584.619	3	1751.848	-2.83
26	n	KmEKR (K94-R98) / VKQK (V327-K330)	K97	K328	661.859	2	1322.71	1.37

Five cross-linked peptide pairs were identified from the analysis of all experimental samples. (*Score*: StavroX score as defined in[4], *Hotspot*: was any of the residues contained in the identified peptide predicted to be a hotspot by Robetta?, *Peptides*: identified peptide sequence, *Crosslinked amino acid (I):* one letter code and pdb number of identified crosslinked amino acid in the interleukin 1 beta, *Crosslinked amino acid (A)*: one letter code and pdb number of identified crosslinked amino acid in the interleukin 1 receptor accessory protein, *m/z*: mass over charge ratio, *z*: charge, *Mass calc.*: calculated mass, *Dev(ppm)*: deviation from the calculated mass in ppm).

Supplementary Table 9: Peptic fragments identified with pepsin digestion of unlabeled proteins and LTQ Orbitrap mass spectrometry analysis.

ProteinSource	Amino Acid Start	Amino Acid Stop	Sequence	MonoIsotopicMass	Z	RT
IL1B	199	217	ESVDPKNYPKKKMEKRFVF	2370.26385	2	15.62
IL1B	250	262	LGGTKGGQDITDF	1308.64302	2	17.26
IL1B	218	228	NKIEINNKLEF	1361.74234	2	19.04
IL1B	163	176	VQGEESNDKIPVAL	1498.77476	2	19.27
IL1B	163	183	VQGEESNDKIPVALGLKEKNL	2281.2398	3	19.3
IL1B	143	158	KALHLQGQDMEQQVVF	1870.94799	2	19.62
IL1B	218	228	NKIEINNKLEF	1361.74234	2	19.66
IL1B	127	142	RDSQQKSLVMSGPYEL	1837.91127	2	20.13
IL1B	218	228	NKIEINNKLEF	1361.74234	2	20.19
IL1B	237	249	YISTSQAENMPVF	1486.68826	2	21.97
IL1B	163	178	VQGEESNDKIPVALGL	1668.88029	2	22
IL1B	159	176	SMSFVQGEESNDKIPVAL	1950.94772	2	23.16
IL1B	227	236	EFESAQFPNW	1254.54258	2	23.43
IL1B	159	178	SMSFVQGEESNDKIPVALGL	2137.04816	2	24.25
IL1B	159	178	SMSFVQGEESNDKIPVALGL	2121.05325	2	25.63
IL1B	237	250	YISTSQAENMPVFL	1599.77232	2	25.66
IL1B	218	228	NKIEINNKLEF	1361.74234	2	34.26
IL1RI	59	81	KDDSKTPVSTEQASRIHQHKEKL	2662.39072	3	13
IL1RI	314	324	AKNTHGIDAAY	1160.56946	2	13.13
IL1RI	170	181	DNIHFSGVKDRL	1400.72809	2	16.55
IL1RI	169	181	LDNIHFSGVKDRL	1513.81215	2	17.79
IL1RI	170	181	DNIHFSGVKDRL	1400.72809	2	17.8
IL1RI	82	94	WFVPAKVEDSGHY	1534.7325	2	19.49
IL1RI	204	215	GKQYPITRVIEF	1450.80528	2	21.35
IL1RI	325	334	IQLIYPVTNF	1207.67214	2	26.72
IL1RAcP	145	153	PVHKLYIEY	1161.63027	2	17.25
IL1RAcP	273	281	LMDSRNEVW	1149.53572	2	17.93
IL1RAcP	168	177	PSSVKPTITW	1115.60954	2	18.99
IL1RAcP	168	178	PSSVKPTITWY	1278.67286	2	20.31

Supplementary Table 10: Differential deuteration states for the 3-way IL1β complex proteins in the following conditions: unbound, bound, and unlabeled.

ProteinSource / startAA_stopAA	Sequence	MonoIsotopicMass	AmountDeut		
			Free	Bound	Unlabeled
IL1B/83_101	ESVDPKNYPKKKMEKRFVF	1185.635557	0.5	0	0
IL1B/102_112	NKIEINNKLEF	681.374807	0.2	0	0
IL1B/121_133	YISTSQAENMPVF	743.8477615	0.1	0	0
IL1B/121_134	YISTSQAENMPVFL	800.3897935	1.2	0.6	0
IL1RI/187_198	GKQYPITRVIEF	725.9062715	0.5	0.3	0

Peptides show decreased amount of deuteration in the bound state with respect to the unbound (free) state. These peptides are indicative of an interface area between proteins.

Supplementary Table 11: Advantages of protein painting compared to existing methods

	PP	CL	HDX	OHF
Experimental set up	Standard	Standard	Optimized for deuterium retention	Optimized for UV pulse shorter than 1 microsecond
Timing of treatment	Short (few minutes)	0.5-2 hours	Short (few minutes)	1 microsecond and shorter
pH conditions	Neutral	Neutral-basic	Strongly acidic (pH=2)	Neutral-slightly basic
Temperature	Room temperature, -20°C for delayed MS analysis	Room temperature, -20°C for delayed MS analysis	Room temperature, 4 °C, and -80 °C	Room temperature, -20°C for delayed MS analysis
Resolution	Half of any trypsin fragment (for two interacting partners, average 4.5 aa, resolution of paint molecules 3 aa)	Restricted to trypsin fragments that contain primary amine, carboxyl, sulfhydryl, or carbonyl groups depending on the cross-linker of choice	Pepsin fragment length, average 10 aa	Half of trypsin fragment with caveat that oxidized arginine might not be cleaved by trypsin
Software	No special requirements: standard ms workflow and software	Dedicated software	Dedicated software	Manually search in the MS spectra for oxidized products
Protein state	Pre-formed complex coated non covalently with small dye molecules	Pre-formed complex covalently crosslinked	Pre-formed complex deuterated	Pre-formed complex oxidized
Output of the method (positive)	Interaction regions are identified by presence of tryptic peptides exclusively derived from both sides of the interface	Binding partners are identified with low specificity for interface solvent excluded binding regions	Interaction regions are identified by a small 1.0073 Dalton shift in peptic fragment peptide mass	Interaction regions are identified by absence of oxidization
Side reaction products / false positives	Within-protein interactions are not identified as false positive because the method is differential (unbound – bound state)	Internal crosslinks, modified peptide (type 0) and cyclic peptide (type 1) are identified as side reaction products	Within-protein interactions are not identified as false positive because the method is differential (unbound – bound state)	OH radical reaction can cause proteins to unfold. Oxidized residues can pre-exist prior to treatment (e.g methionine)
Coverage	Known distribution of trypsin cleavage sites preferred for MS	Protease fragments that contain primary amine, carboxyl, sulfhydryl, or carbonyl groups depending on the cross-linker of choice. Cross-linked lysine will not be cleaved by trypsin.	Pepsin cleavage peptides	Trypsin cleavage sites with possible exception of oxidized Arginine

PP = protein painting; CL = crosslinking; HDX = hydrogen deuterium exchange; OHF = hydroxyl footprinting.

Supplementary Note 1

Conformational changes that affect solvent accessibility for residues that don't belong to the interface are an unlikely source of false positive results in the protein painting method. Such an event has very low probability since the protein painting method is applied to pre-formed protein complexes, for the following reasons.

Analysis of the solvent accessibility of monomeric proteins revealed that few residues (15% in larger proteins) are completely excluded from solvent contact so that the accessible-surface-area (ASA) is effectively zero[7]. Accessibility was defined as the ratio of the residue ASA in the native protein to the ASA it would have in an unfolded and extended polypeptide (Gly-X-Gly, where X is the residue of interest, average ASA in unfolded state=174Å^2). The accessibility threshold was set at 5%, whereas residues with native ASA>5% unfolded ASA were considered on the surface and residues with native ASA <5% unfolded ASA were considered buried in the interior of the protein[7].

In the particular case of K and R residues, partition coefficient measurement and transfer free energy calculations revealed a high propensity of the residues to partition to the surface of the protein[7].

The extent of conformational change in residues not belonging to an interface greatly varies depending on the type of complex that is formed. In particular, conformational changes correlate to the size of complex interface. Analysis of the structural aspects of protein-protein interactions revealed that a typical standard size for the interface area is in the range of 1600 (+/- 400) Å (70% of analyzed proteins)[8].

Proteins that form complexes within the standard size interface undergo small changes in conformation upon complex formation[8]. These small changes in conformation include shifts in surface loops or movements of short segments of peptide chains by up to 1.5 Å and rotation of surface side chains. Approximately 30% of analyzed protein-protein complex presented an interface area larger than 2000 Å. The formation of such complexes involved large changes in conformation of three major types: 1) disorder to order transitions; 2) large movements of the main chain; and 3) in multi-domain proteins, change of the relative position of the domains[8]. Consequently protein-protein complexes with standard size interfaces are unlikely to be associated with a change in solvent accessibility in residues not belonging to protein interface compared to large size interface complexes."

Supplementary References:

1. Ozbabacan, S.E., Engin, H.B., Gursoy, A. & Keskin, O. Transient protein-protein interactions. *Protein Eng. Des. Sel.* **24**, 635-648 (2011).
2. Krissinel, E. & Henrick, K. Inference of macromolecular assemblies from crystalline state. *J. Mol. Biol.* **372**, 774-797 (2007).
3. Thangudu, R.R., Bryant, S.H., Panchenko, A.R. & Madej, T. Modulating protein-protein interactions with small molecules: the importance of binding hotspots. *J. Mol. Biol.* **415**, 443-453 (2012).
4. Götze, M. et al. StavroX--a software for analyzing crosslinked products in protein interaction studies. *J. Am. Soc. Mass. Spectrom.* **23**, 76-87 (2012).
5. Gianazza, E. & Arnaud, P. Chromatography of plasma proteins on immobilized Cibacron Blue F3-GA. Mechanism of the molecular interaction. *Biochem. J.* **203**, 637-641 (1982).
6. Gasymov, O.K. & Glasgow, B.J. ANS fluorescence: potential to augment the identification of the external binding sites of proteins. *Biochim. Biophys. Acta* **1774**, 403-411 (2007).
7. Miller, S., Janin, J., Lesk, A.M. & Chothia, C. Interior and surface of monomeric proteins. *J. Mol. Biol.* **196**, 641-656 (1987).
8. Lo Conte, L., Chothia, C. & Janin, J. The atomic structure of protein-protein recognition sites. *J. Mol. Biol.* **285**, 2177-2198 (1999).